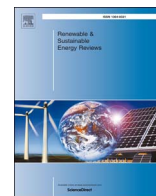




Contents lists available at ScienceDirect

## Renewable and Sustainable Energy Reviews

journal homepage: [www.elsevier.com/locate/rser](http://www.elsevier.com/locate/rser)A review on bismuth telluride ( $\text{Bi}_2\text{Te}_3$ ) nanostructure for thermoelectric applicationsHayati Mamur<sup>a,\*</sup>, M.R.A. Bhuiyan<sup>a</sup>, Fatih Korkmaz<sup>b</sup>, Mustafa Nil<sup>a</sup><sup>a</sup> Department of Electrical and Electronics Engineering, Manisa Celal Bayar University, Manisa, Turkey<sup>b</sup> Department of Electrical and Electronics Engineering, Cankiri Karatekin University, Cankiri, Turkey

## ARTICLE INFO

## Keywords:

Bismuth telluride ( $\text{Bi}_2\text{Te}_3$ )  
 Nanostructure  
 Solvothermal method  
 Thermoelectric generator  
 Thermoelectric application

## ABSTRACT

Bismuth Telluride ( $\text{Bi}_2\text{Te}_3$ ) is basically known as an efficient thermoelectric material. Nowadays, it has been attracted a great deal of interest in energy harvesting, chip cooling, chip sensing and other field of material science because of its potential applications. In order to produce  $\text{Bi}_2\text{Te}_3$  nanostructure, a number of methods such as solvo and hydro thermal, refluxing, straight forward arc-melting and polyol methods have been employed. Among of them, the solvothermal method has been one of the most common methods to fabricate  $\text{Bi}_2\text{Te}_3$  nanostructure in thermoelectric applications. But the development of device-quality material has been a challenging task for the researchers, yet. For this reason, this paper provides a review of current research activities on  $\text{Bi}_2\text{Te}_3$  nanostructure growth by several methods and its characterization through theoretical and analytical aspects. Moreover, the paper handles a systematic and intensive research work to develop and understand the materials in nanostructure forms.

## 1. Introduction

Nanostructure thermoelectric materials have taken attention a great deal of interest because of their potential applications from the thermoelectric generator (TEG) [1–10] to the thermoelectric cooling (TEC) [11–13] and other field of material science [14–17]. They offer excellent opportunities for technological advancements due to their enhanced thermal, electrical and mechanical properties [18–21]. The objective of this paper is to be focused on the enhancing of the feasibility of nanostructure materials having higher thermoelectric figure of merit,  $ZT$ .

In an energy conversion system, nanostructure thermoelectric devices are used for converting thermal energy into electrical energy [22–32]. When a temperature difference,  $\Delta T$  at the sides of a TEG is occurred, it generates a power according to the temperature difference [33]. The power of TEG proportionally and linearly increases with the temperature difference [34]. The converted heat is called as the Seebeck effect. Conversely, a TEC generates a thermal energy when a current is passed through the thermoelement pins, in which case the sides of TEC cools and heats. Namely, when the one side of TEC is cools, then the other side is heats. The phenomenon is known as the Peltier effect [35,36].

Bismuth Telluride ( $\text{Bi}_2\text{Te}_3$ ) is called to one of the best thermoelectric materials since it has a capability to convert waste heat energy into

beneficial electrical energy form [37]. In recent years, many studies have been carried out to obtain high efficiency thermoelectric materials through the development of  $\text{Bi}_2\text{Te}_3$  nanostructure [38–45].

This review paper presents an overview for the remarkable research progress on  $\text{Bi}_2\text{Te}_3$  nanostructure growth by several methods.  $\text{Bi}_2\text{Te}_3$  basically is known as a compound element of Bismuth (Bi) and Tellurium (Te). Bi physically behaves like a metal. But when it is alloyed with Te, then it behaves like an efficient semiconductor thermoelectric type material. It can be used for some applications like as thermoelectric refrigeration, TEG, TEC and other field of material science like as thermal sensor [46–53].  $\text{Bi}_2\text{Te}_3$  and its compounds are the most essential semiconductor thermoelectric materials that employed in state-of-the-art tools, which is operated a temperature range between 200 and 400 K. Their figure of merit,  $ZT = (\alpha^2 \sigma / \kappa) T$ , is around unit [54]. Where,  $\alpha$ ,  $\sigma$  and  $\kappa$  are the Seebeck coefficient, the electric and thermal conductivity, respectively.

Recently, many studies related to their applications have been accomplished in order to enhance the thermoelectric parameters of  $\text{Bi}_2\text{Te}_3$ . When the materials are formed nanostructure dimensions, the figure of merit of them is considerably developed [55–61]. In the present work, a review of  $\text{Bi}_2\text{Te}_3$  nanostructure compounds for thermoelectric applications has been discussed about its growth process by using different methods [62–92]. Ultimately, it has been highlighted that which method would be suitable for growing  $\text{Bi}_2\text{Te}_3$  single crystal

\* Corresponding author.

E-mail address: [hayati.mamur@cbu.edu.tr](mailto:hayati.mamur@cbu.edu.tr) (H. Mamur).<https://doi.org/10.1016/j.rser.2017.10.112>

Received 28 July 2016; Received in revised form 24 September 2017; Accepted 31 October 2017

1364-0321/ © 2017 Elsevier Ltd. All rights reserved.

nanostructure form by using low cost materials.

## 2. Formation of $\text{Bi}_2\text{Te}_3$ nanostructure thermoelectric compounds

There are two approaches for nanostructure formation and fabrication. First of them is the top-down and second of them is the bottom-up approach [93]. The top-down approach includes the achieve splitting of the bulk to nanostructure materials. On the other hand, the bottom-up approach uses the process that nanostructure form is constituted by combining of pieces from bottom up. In some cases, both methods can interfere with one another, which can be called hybrid production.

Nowadays, although the top-down approach has been becoming outdated rapidly, the bottom-up approach has been becoming appreciable in technological applications over a decade. The bottom-up approach produces significantly the best option of executing nanostructures with very low defect record in it and also provides upward to uniform chemical compositions.

Analysis on the characterization and growth of  $\text{Bi}_2\text{Te}_3$  has already utilized both the top-down and the bottom-up approaches in the last decades. In the growth process, these methods are generally classified into two methods, first of them is the physical methods and second of them is the chemical methods. In the growth of  $\text{Bi}_2\text{Te}_3$ , the physical methods basically involve in evaporation, sputtering and spray pyrolysis methods. The chemical synthesis methods include electrochemical, chemical vapor, laser chemical vapor and electrolysis deposition, the hydro and the solvothermal processes.

Because of the necessity of development of alternative materials, the solvothermal reactions have been mainly used to prepare nanostructure form with different morphologies. A solvothermal reaction contains high pressure operations. In order to carry out the targeted material throughout the involved process, the temperature links with the imperative reactions. This process is known to be a fundamental way in order to prepare a nanostructured thermoelectric material. The dimension of crystalline grain, forming of phase and growth of morphology can be easily inspected by using the arrangement process.

## 3. Objectives

As a state-of-the-art bulk thermoelectric material,  $\text{Bi}_2\text{Te}_3$  and its family have better performance compared with bulk counterparts naturally. This review paper focuses on synthesizing and measuring of the structural and optical properties of nanostructure  $\text{Bi}_2\text{Te}_3$  by using various methods. The main goal is to produce thermoelectric nano composites efficiently and cost-effectively. Apart from the nanostructure synthesis, the oxide free material is to develop. In order to obtain better predetermination of thermoelectric performance, the pure  $\text{H}_2$  gas has been used to include various factors such as temperature, pressure etc.  $\text{Bi}_2\text{Te}_3$  nanostructure materials have been used in thermoelectric applications last decades. But the development of device-quality material has been a challenging task for researchers, yet. This calls for undertaking a systematic and intensive research work to develop and understand the material in nanostructure form.

Hence, the objective of the paper is firstly to review the present case of researches on the thermoelectric  $\text{Bi}_2\text{Te}_3$  nanostructures. After that, it is to assess the potentiality of the simple chemical solution processes to synthesis the nanostructures of desired qualities for thermoelectric applications. Lastly, it is to grow the device-quality  $\text{Bi}_2\text{Te}_3$  nanostructures by describing of the synthesis and characterization aspects.

## 4. Literature review

The published new papers on  $\text{Bi}_2\text{Te}_3$  nanomaterial in references have been reviewed to get the main points. The materials and methods in these research papers have been carefully analyzed to make sure the used approaches. Herein, a brief summary of what the paper is about

has been given. Furthermore, it is to focus on objectives/methods/hypotheses of reviewed papers that are being tested according to our previous reports [94,95].

Recently, researchers have attempted to improve the efficiency of  $\text{Bi}_2\text{Te}_3$  materials by creating the nanostructures where one or more dimensions are reduced, such as nano rod, nanowires, nanoplates, nanotubes, nanoflowers and nanosheets etc.

Many research activities on  $\text{Bi}_2\text{Te}_3$  nanostructure were growth by using several processes such as solvothermal, hydrothermal, Bridgman, mechanical alloying, Schlenck, biomolecule-assisted hydrothermal, water-based chemical reduction, chemical oxidation, wet chemical method, refluxing, cryogenic grinding, large-scale zone melting, facile solution. In according to the microstructure properties derived from X-ray diffraction (XRD), scanning electron microscopy (SEM) and transmission electron microscopy (TEM) devices, the solvothermal process is the suitable for growing the  $\text{Bi}_2\text{Te}_3$  nanostructure single crystalline form. The ability to control the size and shape of main materials makes this process versatile, economic, and facile. Therefore, this review is highlighted some advances in nanostructure via solvothermal synthesis process.

Y. Deng et al. [92] reported a solvothermal reaction of Bi (III) chloride dihydrate  $\text{BiCl}_3 \cdot 2\text{H}_2\text{O}$ , Te powder Te, Potassium hydroxide KOH, Potassium borohydride  $\text{KBH}_4$  with the solvent of N, N-dimethyl formamide (DMF) at temperatures between 100 and 180 °C to produce nanocrystalline  $\text{Bi}_2\text{Te}_3$ . They proposed a design approach of  $\text{Bi}_2\text{Te}_3$  nanostructure thermoelectric material. It would be an assembling of two identical processes. In the first process, Te was reduced to  $\text{Te}^{2-}$  and then  $\text{Te}^{2-}$  reacted with  $\text{Bi}^{3+}$ . The second process was a direct combination of metal: Bi ions ( $\text{Bi}^{3+}$ ) would be easily decreased to metal Bi through  $\text{KBH}_4$  to form  $\text{Bi}_2\text{Te}_3$  nanostructures. The product of XRD pattern revealed that the peaks in the patterns corresponded to the reflections of rhombohedral phase with lattice parameters  $a = 4.38 \text{ \AA}$  and  $c = 30.50 \text{ \AA}$ . The X-ray energy dispersive investigation patterns exhibits the existence of Bi and Te peaks. Morphology and crystalline dimension of the synthesized nanostructures were depended on the reaction temperature and time. When the reaction temperature was low and also the time was short, the first process was the dominant formation process and it was easy to form rod-like nanostructures. When the reaction temperature increased or the time was prolonged, the second process would be occurred and the morphology of  $\text{Bi}_2\text{Te}_3$  nanocrystals tended to be sphere shaped. Then, the particle sizes were from 20 to 40 nm. The TEM result demonstrated that the material production obtained at 100 °C for 24 h consisted of mainly nano rods with length  $\sim 150 \text{ nm}$  and average width about 10 nm. The authors showed that in the solvothermal process, the solvent played a crucial role for the nucleation of nanocrystalline materials.

X.B. Zhao et al. [91] prepared a solvothermal synthesis to produce  $\text{Bi}_2\text{Te}_3$  nanoparticles and nanowires by using Bi (III) chloride  $\text{BiCl}_3$  and Te as a precursor with ethylene diamine (EN), dimethyl formamide, pyridine, acetone, ethanol and distilled water respectively. An adequate amount of sodium borohydride  $\text{NaBH}_4$  was included in the solution as the reducing and sodium hydroxide NaOH employed to manage the  $\text{p}^{\text{H}}$  variable of the solution. According to the XRD results, the other additional products were produced metallic Bi, Te and Bismoclite ( $\text{BiOCl}$ ). Distilled water was one of the most prominent solvent for the solvothermal process of  $\text{Bi}_2\text{Te}_3$ . The growth of product in the distilled water was comprised a big nanowire rate with a diameter smaller than 0.1  $\mu\text{m}$  and length of around 10  $\mu\text{m}$ . The experimental results illustrated that the phase propagations, microforms and crystalline dimensions of the nanostructure materials were primarily related to the dielectric constant and surface tension of the solvent employed in this synthesis process. The expected interaction for  $\text{Bi}^{3+}$  ions to accomplice with the decreased  $\text{Te}^{2-}$  ions to compose  $\text{Bi}_2\text{Te}_3$  during this synthesis process, there were other interaction probabilities for  $\text{Bi}^{3+}$  ions such as the diminishment to metallic Bi and the composition of bismoclite when two  $\text{Cl}^-$  ions in  $\text{BiCl}_3$  were changed by some oxide form. If ethanol was

employed, the XRD pattern were found that the phase purity was much better as the response medium than when employing another organic medium, although some little diffraction fluctuations of Bi and Te was.

Y.H. Zhang et al. [90] synthesized a single-phase La-including  $\text{Bi}_2\text{Te}_3$  grounded nanostructures by using a hydrothermal method through the material  $\text{BiCl}_3$ ,  $\text{LaCl}_3$ , selenium (Se) and Te elements like as the reactants,  $\text{NaBH}_4$  like as the reducing,  $\text{NaOH}$  like as the  $\text{p}^{\text{H}}$  variable supervisory and ethylene diamine tetra acetic disodium salt (EDTA) as the dopant. The XRD patterns illustrated that the particles had a single phase rhombohedral form. Since there were no visible diffraction peaks of other elements in the XRD spectra, it was concluded that the spectra had got in the lattice of  $\text{Bi}_2\text{Te}_3$ . A SEM images showed that the micro dimension flower-like agglomerates and petal-like polygons had a diameter of 30 nm and fine crystals. The authors measured the thermoelectric characteristic of the hot-pressed specimens. They affirmed that the characteristics were deeply affected by the imperfections in thermoelectric materials and the substituting lanthanum for the  $\text{Bi}_2\text{Te}_3$  based compound materials was an n-type dopant. Moreover, the experimental results revealed that the substituting of lanthanum could indistinctively enhance the thermoelectric characteristics. The authors also reported a  $ZT$  value of about 0.58 at 480 K.

Y. Xu et al. [89] facilely synthesized  $\text{Bi}_2\text{Te}_3$  nanoplates with around 1  $\mu\text{m}$  in diagonal and 0.1  $\mu\text{m}$  in diameter by using a hydrothermal method in the presence of poly vinyl pyrrolidone (PVP). XRD reflection patterns were easily ranked to a pure rhombohedral phase of  $\text{Bi}_2\text{Te}_3$  with lattice parameters  $a = 4.387 \text{ \AA}$  and  $c = 30.554 \text{ \AA}$ . The products were pure from by indicating the XRD pattern under the current synthesis process. The morphology and crystalline dimension of the samples were determined by SEM and TEM. The low-resolution SEM images revealed that the typical samples consisted of a large extent of plate-like formations. The high-resolution SEM pictures also showed the same formations. The chemical form of these nanoplates indicated that the element ratio of Bi:Te was 38.74:61.26 being the nominal composition. The selective-area electron diffraction (SAED) images consisted of a form, one of the nanoplates, which indicated its single crystalline behavior. The TEM images showed a lot of nanoplates with 0.2–1  $\mu\text{m}$  in diagonal that were strongly in terms of the SEM pictures. The SAED pattern from one of the nanoplates illustrated its single crystalline behavior. Additionally, the experimental results revealed that the nonionic surfactant PVP had a significant role in the crystal growth of  $\text{Bi}_2\text{Te}_3$ . Meanwhile, it was worth mentioning that the morphology of the prepared samples also affected by the temperature. The reaction temperature at 180 °C for 24 h, PVP might affect  $\text{Bi}_2\text{Te}_3$  nuclear to some extent, and some plate-like structures formation. Once reacted at 240 °C for 24 h, too high temperature might destroy the adsorption between  $\text{Bi}_2\text{Te}_3$  nuclear and PVP molecule. Thereby, great deals of crystalline structures were found out during this technique. Consequently, it was recommended that the feasible mission of PVP was to manage the growth rates of separate crystalline faces and ultimately outcome in the construction of  $\text{Bi}_2\text{Te}_3$  nanoplates.

M.M. Nassary et al. [88] prepared single crystalline of  $\text{Bi}_2\text{Te}_3$  by an arranged Bridgman technique, which was constructed locally details in other report [76]. The authors investigated some parameters such as the electrical conductivity depending on temperature difference, the thermoelectric generation, and Hall coefficient for two crystallographic directions. Their results demonstrated that these parameters had anisotropic behaviors. For the particular temperatures, the type of conductivity was determined p-type  $\text{Bi}_2\text{Te}_3$  single crystalline form. Both the Hall coefficient and thermoelectric generation also illustrated the positive sign in behavior. Furthermore, the authors highlighted the temperature dependence of the Hall effect measurement curve behavior for  $\text{Bi}_2\text{Te}_3$  crystal that it consists of three regions. The first region was indicated in the temperature range from 163 to 293 K that represented the extrinsic region. The second region was showed in the temperature range between 293 and 388 K that represented the transition region. The third region was explained at high temperature range between 388

and 528 K that represented the intrinsic region. Lastly, the activation energy was found 0.019 eV. In addition, the energy gap of crystalline was about 0.151 eV. This was the similar in two crystallographic directions as well as ionization energy of 0.036 and 0.0196 eV. The electrical conductivity and Hall effect measurement investigations pointed out that stoichiometric vacancies and some faults were responsible for scattering period. The authors concluded that the semiconductor defects have been occurring at high temperature.

M. Zakeri et al. [87] fabricated  $\text{Bi}_2\text{Te}_3$  nanocrystal via mechanical alloying by using as starting materials of Bi and Te. The authors reported that the nanocrystalline  $\text{Bi}_2\text{Te}_3$  was formed only after 5 h of milling. Results also illustrated that  $\text{Bi}_2\text{Te}_3$  had anisotropic property. Therefore, to obtain the gaining of mean crystalline dimension, the well-known Scherrer formula was applied. The mean grain size of  $\text{Bi}_2\text{Te}_3$  was from 9 to 10 nm after 25 h of milling. Also, the heating of the ball milled samples during differential thermal analysis showed that the synthesized phase was stable up to 500 °C. At the end of milling, after 25 h, the particles had the flaky morphology due to cold working of the smaller particles. At the end of milling, the authors obtained the flaky morphology of crystal structure.

M. Scheele et al. [86] realized a study in order to synthesis  $\text{Bi}_2\text{Te}_3$  nanoparticles by using Schlenck technique at an inert atmosphere condition. The authors prepared 10 nm single crystalline  $\text{Bi}_2\text{Te}_3$  nanoparticles owing to a big reactivity of Bi and Te. The authors also illustrated hydrazine hydrate-based nanoparticles macroscopic pellets. The XRD patterns showed the broadening of the reflections with rhombohedral  $\text{Bi}_2\text{Te}_3$  nanoparticles. Additionally high-resolution scanning electron microscopy (HRSEM) images displayed a little crystal size about 15 nm. Moreover, their SAED measurement results indicated that the fringe patterns were polycrystalline in behavior. Finally, the authors recommended that the thermoelectric characterization of prepared pellets demonstrates a highly decreased thermal and electric conductivity.

Y. Xu et al. [85] reported about the solvothermal method by using the material  $\text{Bi}_2\text{Cl}_3$ , Te,  $\text{NaOH}$ ,  $\text{NaBH}_4$  and the solvent of hexadecyltrimethyl ammonium bromide (CTAB) mixed with distilled water and ethanol. The evaluated data displayed that CTAB had a substantial role on the structure of the plate-like morphology and controlled the growth rates of variable crystalline faces. XRD pattern indicated a pure rhombohedral phase having lattice parameters  $a = 4.435 \text{ \AA}$  and  $c = 30.056 \text{ \AA}$  and produced pure  $\text{Bi}_2\text{Te}_3$ . In their other experimental results, the authors demonstrated that plate-like single crystalline nanoparticles of  $\text{Bi}_2\text{Te}_3$  were produced with from 70 to 200 nm diagonal and 30 nm thicknesses. Furthermore, the morphology of the materials remarkably varied with the help of CTAB during this application. It revealed that typical products consisted of many plate-like crystalline sizes. Besides, the TEM results showed that there were typical nanostructures with about 200 nm in diagonal, which were compatible to the SEM pictures. The authors recommended that the  $\text{Bi}_2\text{Te}_3$  nanostructure production through this route was a very simple technique. By mixing a proper amount of surfactants and regulating the suitable ratio of solvents during the chemical reaction period, the structure and crystalline dimension of production could be easily controlled. At this time, the chemical process solvent took an important role. When water/ethanol was 1:2, even if 0.2 g CTAB was implicated the reaction, plate-like structures were not found. CTAB molecules only showed a role to decrease the dimension of products. By regulating water/ethanol to 1:6, little nanoparticles could be obtained during the technique without CTAB. When CTAB was inserted in the reaction, some plate-like forms come out. Therefore, the authors strongly recommended that the production of  $\text{Bi}_2\text{Te}_3$  single crystal nano plates might comprise two processes: (a) in the initial reaction phase the formation of small  $\text{Bi}_2\text{Te}_3$  nuclei; and (b) plate-like crystal form growth with the help of CTAB molecules under the appropriate situation.

S.H. Kim et al. [84] produced a  $\text{Bi}_2\text{Te}_3$  alloy nanotubes with 1–D structure by interdiffusion at the interface of Bi and Te. The authors

used the material Bi (III) oxide  $\text{Bi}_2\text{O}_3$ , Te dioxide  $\text{TeO}_2$ , which dissolved in Hydrochloric acid HCl and employed as a solvent of Olic acid and Oleylamine at reaction temperature between 160 and 240 °C at a nitrogen atmosphere. Moreover, the authors synthesized the Te nanowire at a temperature of 200 °C with an average diameter from 150 to 200 nm and length from 10 to 15  $\mu\text{m}$ . The Te nanowire was developed into  $\text{Bi}_2\text{Te}_3$  nanotubes conformed by TEM images. Additionally, they observed the Bi and Te crystals in the XRD patterns. The experimental results showed that the hollow structure raised from the void formed of the alloying. Finally, the authors recommended that the aggregation among of the Te nanowires and the diffusion resistance of Te atoms from the inside of the nanowire due to the increase of crystal density hindered the alloying in  $\text{Bi}_2\text{Te}_3$ . However, the alloying into  $\text{Bi}_2\text{Te}_3$  has been expected to be possible if the reduction rate of  $\text{Bi}^{3+}$  decreases.

Q. Zhao and Y.G. Wang [83] obtained the  $\text{Bi}_2\text{Te}_3$  nanostructures. The properties of the nanostructures were several types of morphologies like as needle-shaped nanowires, nanotubes and flakes, and flower-like clusters by using a hydrothermal method. The authors used the  $\text{p}^{\text{H}}$  supervisory like as NaOH, the reducing element like as  $\text{NaBH}_4$  and the other materials  $\text{BiCl}_3$ , Te powder. Their XRD result showed that the reflectivity of the patterns was well ranked to the hexagonal  $\text{Bi}_2\text{Te}_3$ , no notable reflectivity of other phases were defined that indicated the identical form. The flake morphology was shaped via the natural increase of the  $\text{Bi}_2\text{Te}_3$  crystal as demonstrated the SEM image. The production formed irregular flakes having dimensions between 60 and 400 nm. Moreover, the authors recommended the enhancement of the reaction time or temperature. Little parts or flakes steadily lost. But the bigger flakes happened larger and thicker. The TEM images also demonstrated the nanotube with a length up to 700 nm and a diameter between 45 and 64 nm. The needle shaped nanowire with a length up to 2  $\mu\text{m}$  and a diameter of about 50 nm were in good agreement via the SEM images. After that, the other experimental results revealed that  $\text{Bi}_2\text{Te}_3$  nanostructure for one or two dimensional were produced through suitable surfactants at particular temperatures.  $\text{Bi}_2\text{Te}_3$  products having small size formations were an essential thermoelectric material, which was higher figure of merit because of both the scattered of phonons and the improved of the electrical conductivity in interfaces.

Jian-Li Mi et al. [82] carried out the fabrication of  $\text{Bi}_2\text{Te}_3$  thermoelectric nanomaterials by using a simple biomolecule-assisted hydrothermal approach. The authors used the material of  $\text{BiCl}_3$ ,  $\text{K}_2\text{TeO}_3$  which dissolved in alginic acid and finally employed as a solvent of NaOH at reaction temperature 220 °C along 24 h. The product revealed a nanostring-cluster hierarchical structure with a high reaction temperature. It was consisted of a ranked plate-like crystalline in behavior. The plate diameter and thickness were 100 and 10 nm, respectively. The crystalline magnitude and morphology were checked by regulating the density of NaOH affecting a substantial effect on the developing of  $\text{Bi}_2\text{Te}_3$ . Furthermore, the authors also evaluated the thermoelectric parameters like as thermal conductivity, electrical resistivity and Seebeck coefficient at room temperature.

K.T. Kim et al. [81] synthesized  $\text{Bi}_2\text{Te}_3$  nanoparticles by employing the reactants material of  $\text{BiCl}_3$  &  $\text{TeCl}_4$  and the polyol solvent of ethylene glycol. The authors reported that the microstructures of  $\text{Bi}_2\text{Te}_3$  nanoparticles had the 200 nm-sized polycrystalline structures. Besides, the XRD results revealed that the phase of the nanoparticles consisted of mainly  $\text{Bi}_2\text{Te}_3$ . The sintered  $\text{Bi}_2\text{Te}_3$  materials exhibited grain size of 300 nm. Finally, the authors also reported the synthesized material showed extremely the reduced thermal conductivity resulting in an enhanced ZT value of  $\text{Bi}_2\text{Te}_3$  nanoparticles.

M. Salavati-Niasari et al. [80] synthesized that  $\text{Bi}_2\text{Te}_3$  nanoparticle was varied morphologies by means of a hydrothermal process, which was grounded on the reaction between  $\text{Bi}(\text{NO}_3)_3$ ,  $\text{TeCl}_4$  and  $\text{KBH}_4$  in water at different conditions. In this route, the authors used nontoxic precursor and solvent. The XRD patterns corresponded to the reflections of rhombohedral phase  $\text{Bi}_2\text{Te}_3$  having lattice values  $a = 4.38 \text{ \AA}$  and  $c = 30.56 \text{ \AA}$ . The experimental results showed that the synthesized crystals

had diameters ranging between 20 and 25 nm with ultra-high pure form. In addition, the authors were observed that the structures were slightly agglomerated, which reveals temperature effect on morphology of nanostructures. Increasing of the reaction temperature between 120 and 150 °C showed an enhancement of dense agglomerate and crystalline dimension. The X-ray energy dispersive spectroscopy (EDS) results presented that the Bi and Te elements were only exist and the atomic ratio of them in different areas was always 38.63:61.09. The result indicated a phase purity of  $\text{Bi}_2\text{Te}_3$  nanostructure. Ultimately, the authors depicted a novel approach for adjusting the rod and flower like  $\text{Bi}_2\text{Te}_3$ . They asserted that the process was easy, suitable and productive for commercial applications.

C. Kim et al. [79] successfully prepared  $\text{Bi}_2\text{Te}_3$  nanoparticles by applying a water-based chemical reduction process. For the reduction process, some chemicals were utilized a complexion element as an ethylene diamine tetra acetic acid and a reductant element as an ascorbic acid to stable the Bi precursor ( $\text{Bi}(\text{NO}_3)_3$ ) in water and the reaction with the Te powder. The authors were accomplishedly managed a rhombohedral  $\text{Bi}_2\text{Te}_3$  compound with a uniform crystalline size via regulating these reaction elements. The authors also succeeded an average crystalline size around 0.3  $\mu\text{m}$ . Furthermore, they properly carried out a lower thermal conductivity of  $\text{Bi}_2\text{Te}_3$  nanoparticles. Eventually, the entire thermoelectric capability was developed as the figure of merit.

Y. Li et al. [78] synthesized  $\text{Bi}_2\text{Te}_3$  flakes like polyaniline particles. In their experiments, they employed a hydrothermal and a chemical oxidation routes. By using a mechanical blending, the authors produced  $\text{Bi}_2\text{Te}_3$ /polyaniline compounds. In their process, Te powder and  $\text{BiCl}_3$  that inserted in a glass beaker having 140 ml distilled water were used. The  $\text{p}^{\text{H}}$  parameter was regulated by means of NaOH and  $\text{NaBH}_4$ . The XRD results were well ranked to the hexagonal  $\text{Bi}_2\text{Te}_3$ . Additionally, they reported the pure form of  $\text{Bi}_2\text{Te}_3$  because no other remarkable diffractions were found. Furthermore, experiment results showed that the polyaniline powders exhibited the low crystallinity. The SEM images showed of  $\text{Bi}_2\text{Te}_3$  and polyaniline were no uniform flakes having a dimension ranging between 10 and 600 nm. Eventually, the authors indicated that the power factor of  $\text{Bi}_2\text{Te}_3$  was increased by the raised temperature.

Y. Liang et al. [77] employed a simple solvothermal process by using  $\text{Bi}_2\text{O}_3$ , Te that were added to the polyvinylpyrrolidone (PVP) with ethylene glycol solution in order to prepare  $\text{Bi}_2\text{Te}_3$  hexagonal nanostructure without NaOH. According to the author reports, the XRD pattern could be ranked to  $\text{Bi}_2\text{Te}_3$  rhombohedral lattice phase having the lattice values  $a = 4.395 \text{ \AA}$  and  $c = 30.44 \text{ \AA}$ . Therefore, the XRD results illustrated that  $\text{Bi}_2\text{Te}_3$  nanoplates setup this process was formed of  $\text{Bi}_2\text{Te}_3$  rhombohedral lattice phase. After that, the authors showed that the TEM picture of a hexagonal  $\text{Bi}_2\text{Te}_3$  nanoplate was exerted the crystallinity and microstructure of behavior. Other TEM picture showed the single crystalline nature of the nanoplate. In addition, an HRTEM picture revealed the anticipated hexagonal lattice fringes having a lattice spacing of 0.223 nm, which indicated that the formed nanostructures were a single crystalline. Besides, Raman spectrum showed an infrared (IR) active mode within an odd parity. The mode indicated a Raman forbidden structure for a bulk crystalline.

P. Srivastava and K. Singh [76] synthesized  $\text{Bi}_2\text{Te}_3$  nanoparticles (NPs) by utilizing a low-cost wet chemical method at 50 °C. In this experimental procedure, the authors used Te powder,  $\text{BiCl}_3$ , ethylene glycol and hydrazine hydrate chemicals. The XRD and SAED of  $\text{Bi}_2\text{Te}_3$  nanoparticle results revealed the polycrystalline in nature with a rhombohedral structure of the nanocrystallites. The average crystalline size was found to be around 30 nm by using XRD and TEM measurements. The authors obtained a lower thermal conductivity of  $\text{Bi}_2\text{Te}_3$  nanoparticles at room temperature, which obtained the enhanced ZT value.

J. Fu et al. [75] fabricated  $\text{Bi}_2\text{Te}_3$  flower-like nanostructures having a thickness about 20 nm via a cost-efficient hydrothermal technique



having ethylene diamine tetra acetic acid as an additive. They improved the thermoelectric figure of merit 0.7 and the power factor up to  $8.6 \mu\text{W cm}^{-1} \text{K}^{-2}$  of the chemically growth flower-like  $\text{Bi}_2\text{Te}_3$ , which possessed to construct the novel materials and devices related to thermoelectric implementations. Finally, the authors strongly recommended that the nano plates and flower-like  $\text{Bi}_2\text{Te}_3$  nanocrystals (NCs) with no residual additives were unified by high pressure to an n-type nanosized bulk material with protected crystal grain sizes.

S. Gupta et al. [74] prepared  $\text{Bi}_2\text{Te}_3$  nanoparticles by using a refluxing method that was connected to the KOH concentration and the reaction time. The authors used the chemicals with  $\text{BiCl}_3$ , Te powder, EDTA, KOH and  $\text{NaBH}_4$ . Their experimental results displayed the nano rod like structure of  $\text{Bi}_2\text{Te}_3$  with about  $0.1 \mu\text{m}$  length and  $0.02 \mu\text{m}$  diameter. Despite of the varying of concentration of KOH between 0.5 and 1.5 M, these caused the reduced crystalline dimension from 26 to 15 nm. According to the results of the authors, it was suggested that these reaction parameters were played a substantial effect in the developing of nanostructure  $\text{Bi}_2\text{Te}_3$  with different dimension and form.

H.J. Kim et al. [73] prepared a nanostructured thermoelectric  $\text{Bi}_2\text{Te}_3$  powders that have different morphologies through a hydrothermal method, which grounded the reaction with  $\text{BiCl}_3$ , Te, and sodium ethylene diamine tetra acetate ( $\text{Na}_2\text{-EDTA}$ ) at 150, 180 and  $210^\circ\text{C}$ . The XRD patterns of all the diffraction peaks corresponded to the rhombohedral structure that the lattice parameters were  $a = 0.4381 \text{ nm}$  and  $c = 3.046 \text{ nm}$ . The authors reported that these stabilizing agent and temperature factors had a great impact on the morphology of the growth structures. Eventually, the XRD patterns justified that  $\text{Bi}_2\text{Te}_3$  nano plates, nano rods and nanotubes were the same structures. Besides, the TEM image showed the nano plate productions being average edge lengths of 200–800 nm. The morphology of the prepared product was nano rod like with the diameter of 20–80 nm and over  $2 \mu\text{m}$  in length. Finally, the authors recommended that the structure of  $\text{Bi}_2\text{Te}_3$  could be clarified as follows:  $\text{Bi}^{3+}$  ions in the process were controlled by the  $\text{Na}_2\text{-EDTA}$ , while  $\text{Te}^{2-}$  ions were generated from the decreasing of Te by  $\text{NaBH}_4$ . In the process  $\text{Bi}_2\text{Te}_3$  were easily constructed by these  $\text{Bi}^{3+}$  ions and  $\text{Te}^{2-}$  ions.

X. Chen et al. [72] developed  $\text{Bi}_2\text{Te}_3$  nanostructures having an average crystalline dimension around 70 nm by using a cryogenic grinding (CG) method. The authors used a commencing powder mixture, which was composed of  $\text{Bi}_2\text{Te}_3$  coarse nanoparticles around 5 mm by using the novel CG method. The XRD patterns of ingots  $\text{Bi}_2\text{Te}_3$  production for different time duration were shown the high diffraction fluctuations obtained from the database of binary phase. The higher intensity peaks in the pattern of raw ingots demonstrated the existence of texture in the application. The form disappeared as the ingots were grinded into fine powder, which consisted of those peaks weakened. Because of an isotropic form, lattice values were  $a = 0.438 \text{ nm}$  and  $c = 3.049 \text{ nm}$ , and Te–Te layers were connected through the van der Waals forces along c-axis. The resistance of the  $\text{Bi}_2\text{Te}_3$  ingots to divide on non-basal planes was further than that on basal planes. During manufacturing phase, more defects on the basal plane carried out. These were on the non-basal plane leading to the break-down of the long-range lattice order in the direction of c-axis. The authors also compared with other methods being a high-energy ball milling (HEBM) and a spark plasma sintering (SPS) methods. In conclusion, the experimental results indicated that their method could generate  $\text{Bi}_2\text{Te}_3$  powders with finer and better sinter ability.

H. He et al. [71] prepared  $\text{Bi}_2\text{Te}_3$  nanoparticles by the solvothermal method. The raw materials were  $\text{Bi}_2\text{O}_3$ ,  $\text{TeO}_2$ , glycol, NaOH and PVPK-30. The XRD pattern demonstrated the good pure phase of crystal structure and the microform of the prepared samples were a hexagonal lattice having an average crystal dimension of 42 nm. SEM revealed the samples perfect hexagonal nanoparticles obtained from their XRD spectra. The size and thickness of the nanoparticles could be anticipated to be from 400 to 600 and from 40 to 50 nm, respectively. Moreover, the TEM images showed the hexagonal  $\text{Bi}_2\text{Te}_3$  nano sheets at

different magnifications and the structures were seen clearly. The nano sheet clearly obtained the lattice plane with the regular spacing of about 0.37 nm. Additionally, the authors indicated the absorption spectrum, which indicated two peaks about 362 nm (energy 3.43 eV) and 663 nm (energy 1.87 eV). Te electron affinity was defined at 1.97 eV. The electron affinity would be changed by using the formed with Te atoms for  $\text{Bi}_2\text{Te}_3$  nanoparticles. Furthermore, they observed the electron affinity of Te about 663 nm peaks. After that, to verify these results, they conducted an experiment attained the emission spectrum of  $\text{Bi}_2\text{Te}_3$  nano sheets. The application results illustrated a possible setup for the formation of  $\text{Bi}_2\text{Te}_3$  nano sheets were proposed. The formation of faceted nanostructures was connected with selective adsorption of reaction sections and their respective counter ions on the crystal forms during the  $\text{Bi}_2\text{Te}_3$  nanostructure production.

S. Wang et al. [70] prepared a n-type Cu and Zn metal nanostructure arranged  $\text{Bi}_2(\text{Te}_{0.9}\text{Se}_{0.1})_3$  ingots via a large-scale zone melting method. The method had the concept of 'nanoparticle-in-alloy' to separately regulate the electrical and thermal passing features to improve the  $ZT$  value. Cu and Zn elements played multivariate roles in the experiment. Whereas, these were formed metal nano inclusions embedded in van der Waals crystalline boundaries that influenced on thermal parameters. The authors reported that even though the Zn addition acted as weak donor, the density of state effective mass and the Seebeck coefficient noticeably increased and higher the  $ZT$  value was obtained. The authors finally recommended that the substitution of the Cu accommodated in the tetrahedral vacancies form by donating its valence electron and the power factor appreciably optimize. Coupled with the important frustration of heat transferring phonons by Cu nanoinclusions, a highest  $ZT$  value of 1.15 could be accomplish, which was a  $\sim 20\%$  advancement compared with that of commercial other doped ingots. However, the Zn substitution acting as weak donor noticeably raised the density of state effective mass and Seebeck coefficient, and was obtained a high  $ZT$  of 1.1. Especially, the manufacturing process revealed that the high  $ZT$  made metal nanostructure formed n-type materials very promising for commercially thermoelectric applications.

F. Wu et al. [69] synthesized  $\text{Bi}_2\text{Te}_3$  alloy nanostructures having varied morphologies by using a hydrothermal process that had several surfactants. The experimental procedure was mixed in an open beaker. In it, these chemicals were used  $\text{BiCl}_3$ , Te powders/ $(\text{Na}_2\text{TeO}_3$  and  $\text{TeO}_2)$ , EDTA or  $\text{Na}_2\text{-DBS}$  and NaOH. A magnetic stirrer was employed for the mixture, and then  $\text{NaBH}_4$  was introduced into the solution. After that, the XRD patterns showed that all high reflection fluctuations of the applied sample using different Te sources and surfactants were signed to rhombohedral  $\text{Bi}_2\text{Te}_3$  structure and no other noticeably diffractions corresponding to impurity process were obtained. The broadening of the diffraction fluctuations revealed that the specimens were nano sized particle that was consistent with the SEM images. According to the thermoelectric properties, the experimental results showed that the morphologies of the nanostructures had some noticeable changes. Additionally, the authors found a proper micro particle of the bulk pellet. The bulk pellet was provided from flowerlike nanostructures that had a low electrical resistivity and thermal conductivity, large Seebeck coefficient. These gave a high figure of merit  $ZT$  of 1.16. Eventually, the authors asserted that their findings would be helpful for large scale manufacture  $\text{Bi}_2\text{Te}_3$  bulk samples with high  $ZT$  values, because a special method were not needed for the demonstrated process.

Y. Zhang et al. [68] reported the hexagonal nanostructure of  $\text{Bi}_2\text{Te}_3$  single crystals having uniform morphology by using a solvothermal method at lower temperatures. The authors used the raw materials such as  $\text{BiCl}_3$ , Sodium telluride  $\text{Na}_2\text{TeO}_3$ , NaOH, and the kind of surfactants such as PVP-K30, EDTA, CTAB, sodium dodecyl benzene sulfonates (SDBS), ethylene glycol (EG). The authors also obtained the nano sheets by using the solvothermal method depicted a pure rhombohedral structure of  $\text{Bi}_2\text{Te}_3$ . The calculated lattice values were  $a = b = 4.386 \text{ \AA}$  and  $c = 30.482 \text{ \AA}$ . The experimental data clearly explained that high-efficient hexagonal nanostructures obtained, which had a

thickness from 40 to 60 nm and a distance between 400 and 600 nm. These nanostructures exhibited sharp edges indicating a perfect crystallinity behavior. The high-resolution TEM picture clearly demonstrated that the lattice fringes were structurally uniform with a spacing of 0.219 nm. The authors strongly recommended that the microstructural characteristics of the  $\text{Bi}_2\text{Te}_3$  products could be influenced by lots of factors, such as reaction temperature, NaOH concentration, the kind of surfactants, etc. Their experiment gave that the reaction time and temperature, concentration of NaOH, and kinds of surfactants played a crucial role to form  $\text{Bi}_2\text{Te}_3$  nanocrystals. Finally, the authors investigated the transport characteristics of hot pressed bulk samples generated by the as-prepared nano sheets. The thermal resistivity showed importantly an increase owing to the increased phonon scattering at crystalline grain edges.

N. Mntungwa et al. [67] synthesized the monodisperse nanocrystals of  $\text{Bi}_2\text{Te}_3$  capped with alkylamines by utilizing a facile solution based method. The authors used the  $\text{BiCl}_3$ , Bi acetate  $[\text{Bi}(\text{CH}_3\text{COO})_3]$ , Bi nitrate  $[\text{Bi}(\text{NO}_3)_3]$ , Bi carbonate  $[\text{Bi}_2(\text{CO}_3)_2\text{O}_2]$  salts,  $\text{NaBH}_4$ , deionized water, methanol, toluene, hexadecylamine (HDA) and tri-*n*-octylphosphine (TOP) for the  $\text{Bi}_2\text{Te}_3$  and  $\text{Bi}_2\text{Se}_3$  nanocrystal productions. The method involved reduction of Te using sodium borohydride followed by thermolysis in an alkylamine at high temperatures. The authors obtained spherical nanocrystals at all temperatures with hexadecylamine and oleylamine capping agents. The particles were spherical in shape with an average diameter around  $22.27 \pm 5.82$  nm. The corresponding high resolution TEM image presented the microstructure with distinct lattice fringes. The crystalline lattice spacing of about 0.346 nm corresponded to the high intensity planes of rhombohedral crystal structure.

R. Jin et al. [66] synthesized a hierarchical flower-like  $\text{Bi}_2\text{Te}_3$  nanostructure via a solvothermal method. This type of  $\text{Bi}_2\text{Te}_3$  presented good thermoelectrically properties that was suitable for device manufacturing. The authors employed the Bi (III) nitrate pentahydrate  $\text{Bi}(\text{NO}_3)_3 \cdot 5\text{H}_2\text{O}$  and  $\text{Na}_2\text{TeO}_3$ , which dissolved in the water and EG solution. Glucose, NaOH and hydrazine hydrate  $\text{N}_2\text{H}_4 \cdot \text{H}_2\text{O}$  were added into the solution. Herein, the absences of NaOH for  $\text{Bi}_2\text{Te}_3$  nanostructure production were indicated. The XRD pattern of the obtained products demonstrated a rhombohedral phase of  $\text{Bi}_2\text{Te}_3$ . In their study, other crystalline impurities were not detected. These indicate the purity of  $\text{Bi}_2\text{Te}_3$  nanostructure product. Also their SEM images displayed that  $\text{Bi}_2\text{Te}_3$  had a flower-like morphology having the width from 300 to 2000 nm. Moreover, their observations illustrated the flowers composed of smaller nanostructures having the average size of 0.03  $\mu\text{m}$ . Besides, the EDS result gave that two elements of Bi and Te were present with the mole ratio of 38.2: 58.1. In the process, some oxygen also was monitored in the obtained particles that the surface of the products could be oxidized in air. The authors declared that the  $\text{Bi}^{3+}$  ions and  $\text{TeO}_3^{2-}$  anions were firstly reduced for elemental Bi and Te nuclei, respectively. Thereafter, these nuclei behaved with each other to form the tiny  $\text{Bi}_2\text{Te}_3$  crystals. Moreover, the TEM image revealed that the individual nano plate was single crystalline. The concentration of glucose played an important effect in the developing mechanism on structure. Ultimately, according to these results, the ZT value of 0.6 at 600 K was obtained.

E. Ashalley et al. [65] discussed some review studies about the 0D, 1D, 2D and composite  $\text{Bi}_2\text{Te}_3$  nanostructure synthesis and characterization. These studies dialed with experimental and literature about various  $\text{Bi}_2\text{Te}_3$  nanostructures such as nanostructure growing, characterization and other thermoelectric features. The authors used for the implementation of different  $\text{Bi}_2\text{Te}_3$  nano forms by varying the synthesis and characterization processes. These efforts had significant for the increasing the thermoelectric figure-of-merit of the  $\text{Bi}_2\text{Te}_3$  nanostructures and showing from their topological insulating characteristics. Eventually, the authors recommended that  $\text{Bi}_2\text{Te}_3$  and  $\text{Bi}_2\text{Te}_3$ -based nanostructures would be continue leading roles in next generation material manufacturing processes in quantum technology.

L. Yang et al. [64] inspected an n-type hexagonal plate-like  $\text{Bi}_2\text{Te}_3$  nanostructure with uniform morphology by using a solvothermal method and enhanced thermoelectric performance. The authors used  $\text{Bi}_2\text{O}_3$ ,  $\text{TeO}_2$ , NaOH, EG and PVP in order to product  $\text{Bi}_2\text{Te}_3$  nanostructures and as well as indexed exclusively XRD as a rhombohedra phase with lattice constants being  $a = 4.386 \text{ \AA}$  and  $c = 30.478 \text{ \AA}$ . SEM images displayed that  $\text{Bi}_2\text{Te}_3$  had a hexagonal plate-like nanostructures. The lateral size distributions of these nanostructures were varied from a 100 to several 100 nm. Their typical thickness could be observed in the high magnification SEM, which was around 20 nm. These structural features reduced the overall thermal conductivity and in turn led to an improved ZT of 0.88 at 400 K. The authors recommended that the point defects often play an important role for the high frequency phonon vibrating. The authors also concluded that after the sintering, a high-density of little-angle crystalline boundaries managed by a high density of different dislocations is formed due to the stack of plate-like nanostructures along the SPS process. Finally, the authors suggested a strategy to more improve the phonon vibrating of this material.

Y. Liu et al. [63] focused on the role of 0–D defects such as vacancies, interstitials, dopants, and antisites, 1–D defects such as edge and screw dislocations, 2–D defects such as crystalline boundaries and 3–D defects such as nanostructure inclusions in  $\text{Bi}_2\text{Te}_3$  thermoelectric material. The authors strongly proposed that it could have attained its best performance when some defects of the thermoelectric material are eliminated. The thermal and electrical conductivity, Seebeck coefficient are manifestations of charge and phonon flow of their interplay mediated by crystal faults. Their experimental results opened up new alternative opinions for developing high performance thermoelectric materials.

W. Guo et al. [62] prepared a hierarchical  $\text{Bi}_2\text{Te}_3$  nano flowers assembled by 2–D small nanostructures having defects by using a solvothermal process. The authors used some materials such as  $\text{Bi}(\text{NO}_3)_3 \cdot 5\text{H}_2\text{O}$ ,  $\text{Na}_2\text{TeO}_3$ , PVP K30, EG, hydrazine monohydrate  $\text{N}_2\text{H}_4$ , formic acid, ethanol and acetone. The peaks of XRD pattern were well ranked to the rhombohedral  $\text{Bi}_2\text{Te}_3$ . The molar ratio of Bi and Te was well arrangement to be close to 2:3 by using the EDS investigation. Their low-magnification field effecting SEM (FE–SEM) images showed that  $\text{Bi}_2\text{Te}_3$  sample was consisted of nanoflowers. The nanoflowers were setup by curved and inter crossed nanostructures. Moreover, the high-magnification FE–SEM image showed that  $\text{Bi}_2\text{Te}_3$  nanostructures had a diameter ranging between 500 and 600 nm. Its thickness was 16 nm. The authors also achieved the adjustable self-assembly of nano flowers consisted of 2–D thin nano sheets. Eventually, the results showed the maximum ZT value of 0.68 at 475 K. The SEM image provided much more data into the microstructural forms of  $\text{Bi}_2\text{Te}_3$  nano flowers, which were made close-packed nano sheets. The crystalline lattice fringe distances in HRTEM image was 0.31 nm, which was obey with the high intensity  $\text{Bi}_2\text{Te}_3$  planes. The authors finally concluded that the flatness and high efficiency of the defected nano flowers provided a promising way to manage essential contributions to the production of nanotechnology for TEGs and TECs with high yield in a confidential and a repeatable way. Besides, the authors asserted that the Seebeck coefficient could be increased via keeping of thermal conductivity low for more research activities.

When the inspected studies and the future energy requirement of mankind is taken into consideration,  $\text{Bi}_2\text{Te}_3$  is the most important commercial thermoelectric materials [96] that have a relatively higher electrical and a lower thermal conductivity. In recent years, great deals of works [62–92,97–105] have been conducted for  $\text{Bi}_2\text{Te}_3$  nanomaterials. Novel advances in theories and applications have been demonstrated. Its faults could break the sub lattice symmetry as well as it could play an effective role in the electronic scattering methods on the nanostructures. In this communication, how to grow the controllable  $\text{Bi}_2\text{Te}_3$  single crystal nanostructure has been discussed. Additionally, how to increase the thermoelectric performance governed through the

figure of merit  $ZT$  has been researched.

Nanostructured materials with controllable crystalline dimension, shape, crystallinity have attracted due to their unique properties, which are derived mainly from the quantum confinement consequence and large surface-to-volume ratios. The solvothermal synthesis process is treated to be among the most auspicious approaches to prepare nanostructure materials. These processes possess many advantages. They produce an immense amount of nanomaterials at a relatively minimum cost. Also, they have a higher yield owing to well-controlled crystalline dimensions. When the solvothermal process is employed, the thermoelectric performance of nanostructured  $\text{Bi}_2\text{Te}_3$  can be enhanced. The phase purity of the product materials can be easily controlled by varying reaction time at different temperatures. To prepare the  $\text{Bi}_2\text{Te}_3$  nanostructured materials, this process is more suitable compared to other processes. The advantages and disadvantages of the solvothermal synthesis process according to other processes to produce  $\text{Bi}_2\text{Te}_3$  nanostructure material are as follows:

Advantages:

- (1) The solubility of majority materials can be provided by means of heat and pressure applied to up to its crucial point.
- (2) It offers a significant enhancement for the chemical activities of the reactant, the possibility to replace the solid state method, and materials. This may not be carried out by means of a solid state method. Perhaps, it can be occurred by this synthesis process.
- (3) Products of intermediate state, metastable state and specific phase could be easily fulfilled by means of the process. Additionally, novel alloys of metastable state and other specific condensed state could be realized.
- (4) A simplified and sensitive control of the size, structure formation, and the end product crystallinity by the arrangement of parameters such as reaction temperatures and time, the types of solvents, surfactants and precursors can be achieved.
- (5) Substances that are low in melting points and high in vapor pressures and tendency towards pyrolysis would be obtained.

Disadvantages:

- (1) It needs the autoclaves.
- (2) There are some safety problems throughout the reaction process.
- (3) The reaction process cannot be observed.

The unique properties of  $\text{Bi}_2\text{Te}_3$  nanostructure are summarized, which are shown in the Table 1. The growth and characterization parameters of  $\text{Bi}_2\text{Te}_3$  nanostructure are illustrated in Table 2.

## 5. $\text{Bi}_2\text{Te}_3$ nanostructure production techniques

In the  $\text{Bi}_2\text{Te}_3$  nanostructure production, several techniques have been discussed throughout this review paper. According to find out the suitable characterization, these techniques are handled and concluded the recommendation of proper technique to produce the  $\text{Bi}_2\text{Te}_3$

nanostructure.  $\text{Bi}_2\text{Te}_3$  nanostructure production is observed by applying the several growth techniques shown in Table 3.

The solvothermal and hydrothermal technique employed for producing of single phase  $\text{Bi}_2\text{Te}_3$  nanostructure having low crystalline dimension. These techniques have a sensitive control of the crystalline dimension, structure distribution and crystallinity of the end product by the values arrangement such as phase temperatures, time, the used solvent types, surfactants and precursors. According to some earlier reports carried out the authors [106–109], this technique has been quite suitable for the nanostructure material production when comparing with electrochemical synthesis. A majority (~ 80%) of the literature concerning the solvothermal synthesis [110–120] has focused on nanostructure materials. Therefore, this review has been highlighted some of the advances in nanostructure material production by means of the solvothermal or the hydrothermal synthesis.

$\text{Bi}_2\text{Te}_3$  has an alternative way for sustainable energy via extracted from waste heat. It can be usually obtained in nanostructured form by using the state forward arc-melting synthesis technique.  $\text{Bi}_2\text{Te}_3$  compact pellets can be manufactured by employed this technique. Also, the pellets can be easily carried out the electrical properties. However, measurement of microstructural characterization is difficult.

The modified Bridgman technique is locally setup in laboratory. The authors demonstrated to produce single crystals of  $\text{Bi}_2\text{Te}_3$  semiconductor [88]. This method aimed to get a convenient rate of the motion in order to obtain slow cooling rate of crystal growth. The author's investigation involves the thermoelectric properties of single crystal.

The mechanical alloying is high energy powder process [87]. It has been employed to synthesize of nano size powders, lately. This technique was considered by hot processing. To produce nanoparticle by using this technique required hot-pressed in a cylindrical graphite die at high temperature and pressure in vacuum chamber.

$\text{Bi}_2\text{Te}_3$  nanoparticles have been prepared by using the polyol technique with crystalline size from 200 to 300 nm [81]. In this technique, the ethylene glycol (moderately toxic) has been used as the polyol solvent. Everybody is carefully handling this chemical. It should be avoid this chemical for material synthesis. Moreover, it is not possible to produce the low dimensional particle size material by employing this technique.

The water-based chemical reduction process has been started with the chemical oxidation of materials in distilled water by using the ultrasound frequency [79]. The process was designed to be simple but not control the particle size. Moreover, it is not possible to obtain the low dimensional grain and crystalline size of particles.

The chemical oxidation was used to synthesize the  $\text{Bi}_2\text{Te}_3$  composite materials [78]. By using this technique, it is not possible totally oxides free material. The electrical properties cannot be improved by employed this technique.

Based on time dependent experiments, a possible  $\text{Bi}_2\text{Te}_3$  formation mechanism has been suggested by using the wet chemical technique [76]. The concentration of inorganic compound in the solution controls having the disproportionation reaction rate of Te plays an important

**Table 1**  
The unique properties of  $\text{Bi}_2\text{Te}_3$  nanostructure.

Parameter	Properties	References
Crystal structure	Hexagonal-rhombohedral phase	[62,64,66,68,71,76–81,83,85,89,90,92]
Average lattice constant	$a = 4.392 \text{ \AA}$ and $c = 30.438 \text{ \AA}$	[64,68,77,80,85,89,92]
Average crystalline size	~ 97 nm	[71,74,79,81,86,87]
$ZT$ value	0.58 to 1.16	[62,64,66,69,90]
Average diameter	100–600 nm	[62,71,80,84,91]
Average width/length	0.1–15 $\mu\text{m}$	[74,84,91]
Average thickness	10–50 nm	[62,71,80]
Electron affinity	1.87–3.44 eV	[71]
Band gap	~ 0.15 eV	[88]

**Table 2**The growth and characterization parameters of Bi<sub>2</sub>Te<sub>3</sub> nanostructure.

Growth	Main chemicals	Characterization	References
Nanowire	BiCl <sub>3</sub> , Te	XRD, SEM, TEM	[69,73–75,78,83,85,89–91]
Nanostructure	Bi <sub>2</sub> O <sub>3</sub> , Te/TeO <sub>2</sub>	XRD, SEM, TEM, TE Properties	[64,71,77,84]
Nanosheet	BiCl <sub>3</sub> , Na <sub>2</sub> TeO <sub>3</sub> /K <sub>2</sub> TeO <sub>3</sub>	XRD, SEM, TEM	[68,69,82]
Nanoparticle	BiCl <sub>3</sub> /Bi(NO <sub>3</sub> ) <sub>3</sub> , TeCl <sub>4</sub>	XRD, SEM, TEM, TE Properties	[79–81]
Nanoflower	Bi(NO <sub>3</sub> ) <sub>3</sub> ·5H <sub>2</sub> O, Na <sub>2</sub> TeO <sub>3</sub>	XRD, SEM, TEM, EDS, TE Properties	[62,66]
Nanocrystal	BiCl <sub>3</sub> ·2H <sub>2</sub> O, Te	XRD, SEM, TEM	[92]

**Table 3**The different growth techniques and Bi<sub>2</sub>Te<sub>3</sub> nanostructure material production.

Growth technique	Product materials	References
Solvothermal or hydrothermal	Single phase Bi <sub>2</sub> Te <sub>3</sub> nanoparticles with average particle sizes of 15–20 nm	[62,64,66,71,89–92]
Straight forward arc-melting	Highly oriented polycrystals Bi <sub>2</sub> Te <sub>3</sub> nanostructure compact pellets	[99]
Bridgman	Single crystals of Bi <sub>2</sub> Te <sub>3</sub> semiconductor	[88]
Mechanical alloying	Nanocrystalline Bi <sub>2</sub> Te <sub>3</sub> compound with mean grain size ~ 10 nm	[87]
Polyol	Bi <sub>2</sub> Te <sub>3</sub> nanoparticles with crystalline size 200–300 nm	[81]
Water-based chemical reduction	Rhombohedral Bi <sub>2</sub> Te <sub>3</sub> nanoparticles with crystalline size ~ 100 nm	[79]
Chemical oxidation	Bi <sub>2</sub> Te <sub>3</sub> composite materials	[78]
Wet chemical	Bi <sub>2</sub> Te <sub>3</sub> nanoparticles with average grain size ~ 30 nm	[76]
Refluxing	Bi <sub>2</sub> Te <sub>3</sub> nanoparticles that particle size decreases from 23 to 15 nm	[74]
Cryogenic grinding	Bi <sub>2</sub> Te <sub>3</sub> nano sized powders with an average particle size ~70 nm	[72]
Large-scale zone melting	Bi <sub>2</sub> (Te <sub>0.9</sub> Se <sub>0.1</sub> ) <sub>3</sub> ingots found a highest ZT value of 1.15	[70]
Facile solution	Mono disperse nanocrystals of Bi <sub>2</sub> Te <sub>3</sub> with an average diameter of 22.27 nm	[67]

**Table 4**Advantages and disadvantages of Bi<sub>2</sub>Te<sub>3</sub> nanostructure production techniques.

Production Technique	Efficient	Cost-effective	Device-quality	Developed Size	Comments	Reference
Solvothermal or hydrothermal	ZT = 1.16	Low cost	Best	~ 10 nm	Cost effective synthesis	[62,64,66,71,73,75,77,78,80,82,85,89–92]
Straight forward arc-melting	Low	Costly	Fair	Pellets	Difficult to microstructural characterization	[99]
Bridgman	Low	High cost	Fair	Single crystalline	Difficult to device applications	[88]
Mechanical alloying	Medium	Costly	Good	~ 10 nm	Required high temperature and pressure	[87]
Polyol	Medium	Medium Cost	Poor	~ 200 nm	Use the toxic chemical	[81]
Water-based chemical reduction	Low	Medium Cost	Poor	~ 300 nm	Do not control the particle size	[79]
Chemical oxidation	Low	Medium Cost	Poor	Not uniform	Electrical properties cannot be improved	[78]
Wet chemical	Medium	Low cost	Good	~ 30 nm	Use the toxic chemical	[76,79]
Refluxing	Medium	Costly	Good	~ 15 nm	Handled so much carefully	[74]
Cryogenic grinding	Medium	Costly	Poor	~ 70 nm	May not be suitable for device manufacturing	[72]
Large-scale zone melting	ZT = 1.15	Costly	Good	Nanostructure	Difficult to microstructural characterization	[70]
Facile solution	Medium	Costly	Fair	~ 22 nm	Use the toxic chemical	[67]

role in the formation of the Bi<sub>2</sub>Te<sub>3</sub>. In this technique, ethylene glycol has been sequentially added for solution preparation. Toxicity and death may occur even after drinking a small amount ethylene glycol.

Bi<sub>2</sub>Te<sub>3</sub> nanoparticles were prepared by the refluxing technique in different conditions such as varying concentration of KOH and reaction timing [74]. During this technique, some of reaction chemicals (Te and BiCl<sub>3</sub>) are mildly toxic, so need to be handled carefully. After the formation of nanoparticles, the surfactant ethylene diamine tetra acetic acid acts as a structure directing agent, also can induce the growth mechanism and direction of nucleation to form different structure.

The cryogenic grinding technique has been used for rapid Bi<sub>2</sub>Te<sub>3</sub> production having nano sized powders [72]. During this technique, Bi<sub>2</sub>Te<sub>3</sub> was possibility to transform into non-equilibrium amorphous decomposed or phase formation. This technique might not be appropriate applicable for producing of Bi<sub>2</sub>Te<sub>3</sub> nanostructure materials.

The large-scale zone melting technique has been suitable for producing of Bi<sub>2</sub>Te<sub>3</sub> ingot [70]. Compared with other techniques, it is not

suitable for producing of Bi<sub>2</sub>Te<sub>3</sub> nanostructure. For microstructural investigation, the ingot is complicated to different measurements.

The facile solution technique has been applicable for producing of Bi<sub>2</sub>Te<sub>3</sub> one-dimensional nano rod [67]. Herein, the technique uses the ethylene diamine tetra acetic acid as an additive. The chemical exhibits low acute toxicity in aqueous solution. For producing of Bi<sub>2</sub>Te<sub>3</sub> nanostructure need to be handled carefully. Advantages and disadvantages of Bi<sub>2</sub>Te<sub>3</sub> nanostructure production techniques are presented on Table 4.

Compared with different techniques in view of producing of Bi<sub>2</sub>Te<sub>3</sub> nanostructure, it has been concluded that the solvothermal or the hydrothermal technique can produce finer and device quality single phase Bi<sub>2</sub>Te<sub>3</sub> nanostructure powders that applicable for thermoelectric device manufacturing applications. These are the cost effective synthesis techniques.



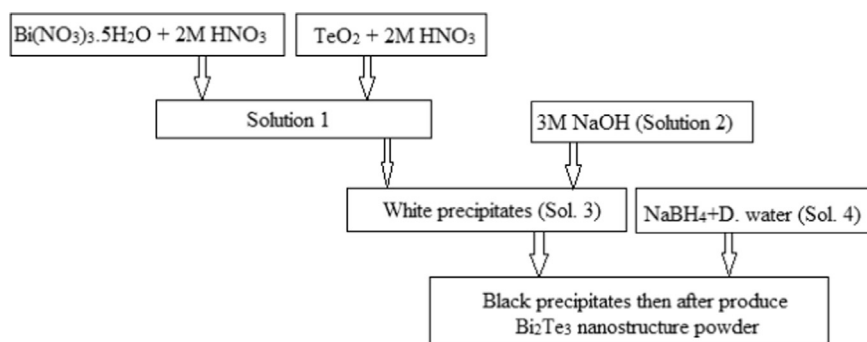
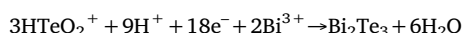
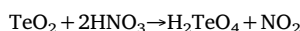


Fig. 1. The schematic drawing of the recommended the solvothermal process.

## 6. Conclusion and future research

In conclusion, the figure of merit,  $ZT$  increases from 0.58 to 1.16 when the materials are developed in nanostructure form. In this review paper, the main material using  $\text{Bi}(\text{NO}_3)_3 \cdot 5\text{H}_2\text{O}$  and  $\text{TeO}_2$  in the solvothermal method was proposed to grow a controllable  $\text{Bi}_2\text{Te}_3$  single crystal nanostructure for thermoelectric applications in accordance the synthesizing aspects.  $\text{Bi}_2\text{Te}_3$  nanostructures were synthesized by this process utilizing the different concentration of  $\text{HNO}_3$  and  $\text{NaOH}$  with or without  $\text{NaBH}_4$ . Since the compounds are ecological behavior with low toxicity and cost, stability in air, commercial availability and easy of handling properties. Many researchers used  $\text{KOH}$  and other materials to prepare some solutions. Here, Nitric Acid,  $\text{HNO}_3$  instead of these materials was firstly recommended in order preparing the solution. Then,  $\text{TeO}_2$  powder could be dissolved in  $\text{HNO}_3$  according to the recommended process. After that,  $\text{Bi}(\text{NO}_3)_3 \cdot 5\text{H}_2\text{O}$  material could be added at  $80^\circ\text{C}$  and dissolved accompanied by magnetic stirring and consequently completed the other treatments to produce single crystal  $\text{Bi}_2\text{Te}_3$  nanostructure. The estimated possible chemical reactions were given under as follow:



The two upper metallic solutions were reserved in one flux (sol. 1) and other flux was fulfilled with  $\text{NaOH}$  solution (sol. 2). These two solutions were mixed together at room temperature with adjusting the hydro–dynamic atmosphere. Then, a complete co–precipitation was developed by magnetic stirring for half an hour and developed the white precipitates. The Bi and Te oxides were eliminated by using  $\text{NaBH}_4$ . Some white precipitate was reserved in a borosilicate flux (sol. 3) at temperature by using the magnetic stirrer for several minutes. Other flux was carried out by means of  $\text{NaBH}_4$  solution with distilled water at temperature soluble by a magnetic stirrer during several minutes (sol. 4). The sol. 3 and sol. 4 were mixed together at temperature with adjusting the hydro–dynamic atmosphere. The schematic drawing of the recommended the solvothermal process is shown Fig. 1.

The complete co–precipitation was developed by a magnetic stirrer for several hours to remove the oxidization. The developed precipitates were collected by a centrifugation, washed several times with distilled water and pure ethanol and finally dried by heat for several hours in an oven. Then, the dried precursor was calcined in a vacuum furnace for several hours. After that, the  $\text{Bi}_2\text{Te}_3$  powder was developed. Lastly, in order to produce oxide free sample, a computer controlled pure  $\text{H}_2$  gas was passed throughout the sample. It was concluded by using this process, which the ultra–fine device quality materials would be produced for thermoelectric applications. In accordance the characterizing aspects such as XRD, SEM, and TEM the solvothermal process has also the suitable for growing the  $\text{Bi}_2\text{Te}_3$  nanostructure form.

Further research will be recommended to study the thermoelectric

properties of  $\text{Bi}_2\text{Te}_3$  nanostructures to improve the Seebeck coefficient while keeping the thermal conductivity low and the electrical conductivity high.

## Acknowledgements

This work was supported by the Scientific & Technological Research Council of Turkey under grant of TUBİTAK 2221 Fellowship Program, Ref No: 21514107–115.02–E.69236 and Manisa Celal Bayar University Scientific Research Projects Coordination Unit, No: 2016–147.

## References

- [1] Ahiska R, Mamur H. Development and application of a new power analyzes system for testing of geothermal thermoelectric generators. *Int J Green Energy* 2015;13:672–81.
- [2] Ahiska R, Mamur H. Design and implementation of a new portable thermoelectric generator for low geothermal temperatures. *IET Renew Power Gen* 2013;7:700–6.
- [3] Siddique AR, Mahmud S, Van Heyst B. A review of the state of the science on wearable thermoelectric power generators (TEGs) and their existing challenges. *Renew Sustain Energy Rev* 2017;73:730–44.
- [4] Champier D. Thermoelectric generators: a review of applications. *Energy Convers Manag* 2017;140:167–81.
- [5] Ng IK, Kok KY, Rahman CC, Choo TF, Saidin NU. Bismuth telluride based nano-wires for thermoelectric power generation. *Mater Today* 2016;3:533–7.
- [6] Smith CJ, Cahill JS, Nuhoglu A. Macro to nano: scaling effects of  $\text{Bi}_2\text{Te}_3$  thermoelectric generators for applications in space. *PAM Rev: Energy Sci Technol* 2016;3:86–99.
- [7] Alptekin M, Calisir T, Baskaya S. Design and experimental investigation of a thermoelectric self–powered heating system. *Energy Convers Manag* 2017;146:244–52.
- [8] Gupta M. Review on heat recovery unit with thermoelectric generators. *Int J Eng Innov Technol (IJETT)* 2014;4:128–31.
- [9] Ding LC, Akbarzadeh A, Tan L. A review of power generation with thermoelectric system and its alternative with solar ponds. *Renew Sustain Energy Rev* 2018;81:799–812.
- [10] Huen P, Daoud WA. Advances in hybrid solar photovoltaic and thermoelectric generators. *Renew Sustain Energy Rev* 2017;72:1295–302.
- [11] Sajid M, Hassan I, Rahman A. An overview of cooling of thermoelectric devices. *Renew Sustain Energy Rev* 2017;78:15–22.
- [12] Ahiska R, Dislitas S. Computer controlled test system for measuring the parameters of the real thermoelectric module. *Energy Convers Manag* 2011;52:27–36.
- [13] Ahiska R, Dislitas S, Omer G. A new method and computer–controlled system for measuring the time constant of real thermoelectric modules. *Energy Convers Manag* 2012;53:314–21.
- [14] Kishore RA, Priya S. A review on design and performance of thermomagnetic devices. *Renew Sustain Energy Rev* 2018;81:33–44.
- [15] Ovik R, Long BD, Barma MC, Riaz M, Sabri MF, Said SM, Saidur R. A review on nanostructures of high–temperature thermoelectric materials for waste heat recovery. *Renew Sustain Energy Rev* 2016;64:635–59.
- [16] Burmester D, Rayudu R, Seah W, Akinyele D. A review of nanogrid topologies and technologies. *Renew Sustain Energy Rev* 2017;67:760–75.
- [17] Bhowmik C, Bhowmik S, Ray A, Pandey KM. Optimal green energy planning for sustainable development: a review. *Renew Sustain Energy Rev* 2017;71:796–813.
- [18] Siouane S, Jovanović S, Poure P. Fully electrical modeling of thermoelectric generators with contact thermal resistance under different operating conditions. *J Electron Mater* 2017;46:40–50.
- [19] Oh JY, Lee JH, Han SW, Chae SS, Bae EJ, Kang YH, Choi WJ, Cho SY, Lee JO, Baik HK, Lee TI. Chemically exfoliated transition metal dichalcogenide nanosheet–based wearable thermoelectric generators. *Energy Environ Sci* 2016;9:1696–705.
- [20] Liu D, Peng W, Li Q, Gao H, Jin AJ. Preparation and characterization of segmented stacking for thermoelectric power generation. *Clean Technol Environ* 2016;18:1203–10.

- [21] Bianchini A, Donini F, Pellegrini M, Saccani C. Techno-economic analysis of different plant configuration for thermoelectric cogeneration from biomass boiler. *Int J Renew Energy Res* 2016;6:1565–73.
- [22] Mamur H, Ahiska R. Application of a DC–DC boost converter with maximum power point tracking for low power thermoelectric generators. *Energy Convers Manag* 2015;97:265–72.
- [23] Schönherr P, Tilbury T, Wang H, Haghighirad AA, Srot V, Van Aken PA, Hesjedal T. Correction to step-flow growth of  $\text{Bi}_2\text{Te}_3$  nanobelts. *Cryst Growth Des* 2017;17:1438.
- [24] Huang H, Li Q, Qian Y, Xu C. Widely tunable band gap of the quantum-confined bismuth telluride nanocrystals. *J Nanoelectron Optoelectron* 2017;12:205–8.
- [25] Rashad MM, El-Dissouky A, Soliman HM, Elseman AM, Refaat HM, Ebrahim A. Structure evaluation of bismuth telluride ( $\text{Bi}_2\text{Te}_3$ ) nanoparticles with enhanced Seebeck coefficient and low thermal conductivity. *Mater Res Innov* 2017;1–9.
- [26] Twaha S, Zhu J, Yan Y, Li B. A comprehensive review of thermoelectric technology: materials, applications, modelling and performance improvement. *Renew Sustain Energy Rev* 2016;65:698–726.
- [27] Angeline AA, Jayakumar J, Asirvatham LG. Performance analysis of ( $\text{Bi}_2\text{Te}_3$ –PbTe) hybrid thermoelectric generator. *Int J Power Electron Drive Syst (IJPEDS)* 2017;8:917–25.
- [28] Lee J, Lim C, Lim J, Yang S, Im J. Application of solar thermoelectric generation system for health monitoring system of civil infrastructures. *KSCE J Civ Eng* 2017;1–7.
- [29] Omer G, Yavuz AH, Ahiska R. Heat pipes thermoelectric solar collectors for energy applications. *Int J Hydrog Energy* 2017;42:8310–3.
- [30] Angeline AA, Jayakumar J, Asirvatham LG, Marshal JJ, Wongwises S. Power generation enhancement with hybrid thermoelectric generator using biomass waste heat energy. *Exp Therm Fluid Sci* 2017;85:1–12.
- [31] Al-Nimr MA, Tashtoush BM, Jaradat AA. Modeling and simulation of thermoelectric device working as a heat pump and an electric generator under Mediterranean climate. *Energy* 2015;90:1239–50.
- [32] Guan M, Wang K, Xu D, Liao WH. Design and experimental investigation of a low-voltage thermoelectric energy harvesting system for wireless sensor nodes. *Energy Convers Manag* 2017;138:30–7.
- [33] Ahiska R, Mamur H. A test system and supervisory control and data acquisition application with programmable logic controller for thermoelectric generators. *Energy Convers Manag* 2012;64:15–22.
- [34] Ahiska R, Mamur H, Ullis M. Modeling and experimental study of thermoelectric module as generator. *J Fac Eng Archit Gaz* 2011;26:889–96.
- [35] Verbelen Y, De Winne S, Blondeel N, Peeters A, Braeken A, Touhafi A. Analysis of thermoelectric coolers as energy harvesters for low power embedded applications. *World Acad Sci Eng Technol Int J Electr Comput Eng Electron Commun Eng* 2017;11:279–86.
- [36] Dey A, Bajpai OP, Sikder AK, Chattopadhyay S, Khan MAS. Recent advances in CNT/graphene based thermoelectric polymer nanocomposite: a proficient move towards waste energy harvesting. *Renew Sustain Energy Rev* 2016;53:653–71.
- [37] Culebras M, Uriol B, Gómez CM, Cantarero A. Controlling the thermoelectric properties of polymers: application to PEDOT and polypyrrole. *Phys Chem Chem Phys* 2015;17:15140–5.
- [38] Antonenko AO, Charnaya EV, Nefedov DY, Podorozhkin DY, Uskov AV, Bugaev AS, Lee MK, Chang LJ, Naumov SV, Perevozchikova YA, Chistyakov VV, Marchenkova EB, Weber HW, Huang JCA, Marchenkov VV. NMR studies of single crystals of the topological insulator  $\text{Bi}_2\text{Te}_3$  at low temperatures. *Phys Solid State* 2017;59:855–9.
- [39] Luo B, Deng Y, Wang Y, Gao M, Zhu W, Hashim HT, García-Cañadas J. Synergistic photovoltaic–thermoelectric effect in a nanostructured CdTe/ $\text{Bi}_2\text{Te}_3$  heterojunction for hybrid energy harvesting. *RSC Adv* 2016;6:114046–51.
- [40] Wu K, Yan Y, Zhang J, Mao Y, Xie H, Yang J, Zhang Q, Uher C, Tang X. Preparation of n-type  $\text{Bi}_2\text{Te}_3$  thermoelectric materials by non-contact dispenser printing combined with selective laser melting. *Phys Status Solidi–R* 2017.
- [41] Zhang C, Fan XA, Hu J, Jiang C, Xiang Q, Li G, Li Y, He Z. Changing the band gaps by controlling the distribution of initial particle size to improve the power factor of n-type  $\text{Bi}_2\text{Te}_3$  based polycrystalline bulks. *Adv Eng Mater* 2017.
- [42] Gaul A, Peng Q, Singh DJ, Ramanath G, Borca-Tasciuc T. Pressure-induced insulator-to-metal transitions for enhancing thermoelectric power factor in bismuth telluride-based alloys. *Phys Chem Chem Phys* 2017;19:12784–93.
- [43] Mahmud KH, Yudistirani SA, Ramadhan AI. Analysis of power characteristics of model thermoelectric generator (TEG) small modular. *Int J Sci Technol Res* 2017;6:161–7.
- [44] Lee CW, Kim GH, Choi JW, An KS, Kim JS, Kim H, Lee YK. Improvement of thermoelectric properties of  $\text{Bi}_2\text{Te}_3$  and  $\text{Sb}_2\text{Te}_3$  films grown on graphene substrate. *Phys Status Solidi–R* 2017;170029–32.
- [45] Culebras M, Igual-Muñoz AM, Rodríguez-Fernández C, Gómez-Gómez MI, Gomez C, Cantarero A. Manufacturing Te/PEDOT films for thermoelectric applications. *ACS Appl Mater Interfaces* 2017.
- [46] Gaikwad M, Shevade D, Kadam A, Subham B. Review on thermoelectric refrigeration: materials and technology. *Int J Curr Eng Technol* 2016;4:67–71.
- [47] Akshay VR, Suneesh MV, Vasundhara M. Tailoring thermoelectric properties through structure and morphology in chemically synthesized n-type bismuth telluride nanostructures. *Inorg Chem* 2017. [May 10].
- [48] Jian SR, Le PH, Luo CW, Juang YJ. Nanomechanical and wettability properties of  $\text{Bi}_2\text{Te}_3$  thin films: effects of post-annealing. *J Appl Phys* 2017;121:175302–5.
- [49] Talebi T, Ghomashchi R, Talemi P, Aminorroaya S. Preparation of n-type  $\text{Bi}_2\text{Te}_3$  Films by electrophoretic deposition. *Int J Chem Mol Nucl Mater Metall Eng* 2017;11:257–60.
- [50] Erickson KJ, Limmer SJ, Yelton WG, Rochford C, Siegal MP, Medlin DL. Evolution of microstructural disorder in annealed bismuth telluride nanowires. *ECS J Solid State Sci* 2017;6:N3117–24.
- [51] Fang H, Bahk JH, Feng T, Cheng Z, Mohammed AM, Wang X, Ruan X, Shakouri A, Wu Y. Thermoelectric properties of solution-synthesized n-type  $\text{Bi}_2\text{Te}_3$  nanocomposites modulated by Se: an experimental and theoretical study. *Nano Res* 2016;9:117–27.
- [52] Loa I, Bos JW, Downie RA, Syassen K. Atomic ordering in cubic bismuth telluride alloy phases at high pressure. *Phys Rev B* 2016;93:224109.
- [53] Sharma S, Schwingenschlög U. Thermoelectric response in single quintuple layer  $\text{Bi}_2\text{Te}_3$ . *ACS Energy Lett* 2016;1:875–9.
- [54] Brostow W, Datashvili T, Lobland HEH, Hilbig T, Su L, Vinado C, White J. Bismuth telluride-based thermoelectric materials: coatings as protection against thermal cycling effects. *J Mater Res* 2012;27:2930–6.
- [55] Hines M, Lenhardt J, Lu M, Jiang L, Xiao Z. Cooling effect of nanoscale  $\text{Bi}_2\text{Te}_3/\text{Sb}_2\text{Te}_3$  multilayered thermoelectric thin films. *J Vac Sci Technol A* 2012;30:041509.
- [56] Khodiri AA, Nawar AM, El-kader KA. Effect of x-ray irradiation on structural and optical properties of topological insulator bismuth telluride nano-structure thin film. *J Appl Phys* 2016;8:60–8.
- [57] Gupta A, Chand S, Patel NK, Soni A. A review on thermoelectric cooler. *Int J Innov Res Sci Technol* 2016;2:674–9.
- [58] Orr B, Akbarzadeh A, Mochizuki M, Singh R. A review of car waste heat recovery systems utilising thermoelectric generators and heat pipes. *Appl Therm Eng* 2016;101:490–5.
- [59] Rodríguez-Fernández C, Manzano CV, Romero AH, Martín J, Martín-González M, de Lima Jr MM, Cantarero A. The fingerprint of Te-rich and stoichiometric  $\text{Bi}_2\text{Te}_3$  nanowires by raman spectroscopy. *Nanotechnology* 2016;27:075706.
- [60] Goldsmid HJ. Bismuth telluride and its alloys as materials for thermoelectric generation. *Materials* 2014;7:2577–92.
- [61] Saleemi M, Toprak MS, Li S, Johnsson M, Muhammed. Synthesis, processing, and thermoelectric properties of bulk nanostructured bismuth telluride ( $\text{Bi}_2\text{Te}_3$ ). *J Mater Chem* 2012;22:725–30.
- [62] Guo W, Ma J, Zheng W.  $\text{Bi}_2\text{Te}_3$  nanoflowers assembled of defective nanosheets with enhanced thermoelectric performance. *J Alloy Compd* 2016;659:170–7.
- [63] Liu Y, Zhou M, He J. Towards higher thermoelectric performance of  $\text{Bi}_2\text{Te}_3$  via defect engineering. *Scr Mater* 2016;111:39–43.
- [64] Yang L, Chen ZG, Hong M, Han G, Zou J. Enhanced thermoelectric performance of nanostructured  $\text{Bi}_2\text{Te}_3$  through significant phonon scattering. *ACS Appl Mater Interfaces* 2015;7:23694–9.
- [65] Ashalley E, Chen H, Tong X, Li H, Wang ZM. Bismuth telluride nanostructures: preparation, thermoelectric properties and topological insulating effect. *Front Mater Sci* 2015;9:103–25.
- [66] Jin R, Liu J, Li G. Facile solvothermal synthesis, growth mechanism and thermoelectric property of flower-like  $\text{Bi}_2\text{Te}_3$ . *Cryst Res Technol* 2014;49:460–6.
- [67] Mntungwa N, Rajasekhar PVSR, Ramasamy K, Revaprasadu N. A simple route to  $\text{Bi}_2\text{Se}_3$  and  $\text{Bi}_2\text{Te}_3$  nanocrystals. *Superlattices Microstruct* 2014;69:226–30.
- [68] Zhang Y, Hu LP, Zhu TJ, Xie J, Zhao XB. High yield  $\text{Bi}_2\text{Te}_3$  single crystal nanosheets with uniform morphology via a solvothermal synthesis. *Cryst Growth Des* 2013;13:645–51.
- [69] Wu F, Song H, Gao F, Shi W, Jia J, Hu X. Effects of different morphologies of  $\text{Bi}_2\text{Te}_3$  nanopowders on thermoelectric properties. *J Electron Mater* 2013;42:1140–5.
- [70] Wang S, Li H, Lu R, Zheng G, Tang X. Metal nanoparticle decorated n-type  $\text{Bi}_2\text{Te}_3$ -based materials with enhanced thermoelectric performances. *Nanotechnology* 2013;24:285702.
- [71] He H, Huang D, Zhang X, Li G. Characterization of hexagonal  $\text{Bi}_2\text{Te}_3$  nanosheets prepared by solvothermal method. *Solid State Commun* 2012;152:810–5.
- [72] Chen X, Liu L, Dong Y, Wang L, Chen L, Jiang W. Preparation of nano-sized  $\text{Bi}_2\text{Te}_3$  thermoelectric material powders by cryogenic grinding. *Prog Nat Sci: Mater Int* 2012;22:201–6.
- [73] Kim HJ, Han MK, Kim HY, Lee W, Kim SJ. Morphology controlled synthesis of nanostructured  $\text{Bi}_2\text{Te}_3$ . *Bull Korean Chem Soc* 2012;33:3977–80.
- [74] Gupta S, Neelshwar S, Kumar V, Chen YY. Synthesis of bismuth telluride nanostructures by refluxing method. *Adv Mater Lett* 2012;3:50–4.
- [75] Fu J, Song S, Zhang X, Cao F, Zhou L, Li X, Zhang H.  $\text{Bi}_2\text{Te}_3$  nanoplates and nanoflowers: synthesized by hydrothermal process and their enhanced thermoelectric properties. *Cryst Eng Comm* 2012;14:2159–65.
- [76] Srivastava P, Singh K. Structural and thermal properties of chemically synthesized  $\text{Bi}_2\text{Te}_3$  nanoparticles. *J Therm Anal Calorim* 2012;110:523–7.
- [77] Liang Y, Wang W, Zeng B, Zhang G, Huang J, Li J, Li T, Song Y, Zhang X. Raman scattering investigation of  $\text{Bi}_2\text{Te}_3$  hexagonal nanoplates prepared by a solvothermal process in the absence of NaOH. *J Alloy Compd* 2011;509:5147–51.
- [78] Li Y, Zhao Q, Wangn Y, Bi K. Synthesis and characterization of  $\text{Bi}_2\text{Te}_3$  polyaniline composites. *Mater Sci Semicond Process* 2011;14:219–22.
- [79] Kim C, Kim DH, Han YS, Chung JS, Park SH, Kim H. Fabrication of bismuth telluride nanoparticles using a chemical synthetic process and their thermoelectric evaluations. *Powder Technol* 2011;214:463–8.
- [80] Niasaria MS, Bazarganipour M, Davar F. Hydrothermal preparation and characterization of based-alloy  $\text{Bi}_2\text{Te}_3$  nanostructure with different morphology. *J Alloy Compd* 2010;489:530–4.
- [81] Kim KT, Lee HM, Kim DW, Kim KJ, Ha GH. Bismuth–telluride thermoelectric nanoparticles synthesized by using a polyol process. *J Korean Phys Soc* 2010;57(4):1037–40.
- [82] Mi JL, Lock N, Sun T, Christensen M, Sondergard M, Hald P, Hng HH, Ma J, Iversen BB. Biomolecule-assisted hydrothermal synthesis and self-assembly of  $\text{Bi}_2\text{Te}_3$  nanostructuring-cluster hierarchical structure. *ACS Nano* 2010;4:2523–30.
- [83] Zhao Q, Wang YG. A facile two-step hydrothermal route for the synthesis of

- low-dimensional structured  $\text{Bi}_2\text{Te}_3$  nanocrystals with various morphologies. *J Alloy Compd* 2010;497:57–61.
- [84] Kim SH, Park BK. Solvothermal synthesis of  $\text{Bi}_2\text{Te}_3$  nanotubes by the interdiffusion of Bi and Te metals. *Mater Lett* 2010;64:938–41.
- [85] Xu Y, Ren Z, Cao G, Ren W, Dang K, Zhong Y. Fabrication and characterization of  $\text{Bi}_2\text{Te}_3$  nanoplates via a simple solvothermal process. *Physica B* 2009;404:4029–33.
- [86] Scheele M, Oeschler N, Meier K, Kornowski A, Klinke C, Weller H. Synthesis and thermoelectric characterization of  $\text{Bi}_2\text{Te}_3$  nanoparticles. *Adv Funct Mater* 2009;19:3476–83.
- [87] Zakeri M, Allahkarami M, Kavei G, Khanmohammadian A, Rahimpour MR. Synthesis of nanocrystalline  $\text{Bi}_2\text{Te}_3$  via mechanical alloying. *J Mater Process Technol* 2009;209:96–101.
- [88] Nassary MM, Shaban HT, El-Sadek MS. Semiconductor parameters of  $\text{Bi}_2\text{Te}_3$  single crystal. *Mater Chem Phys* 2009;113:385–8.
- [89] Xu Y, Ren Z, Ren W, Cao G, Dang K, Zhong Y. Hydrothermal synthesis of single-crystalline  $\text{Bi}_2\text{Te}_3$  nanoplates. *Mater Lett* 2008;62:4273–6.
- [90] Zhang YH, Zhua TJ, Tu JP, Zhao XB. Flower-like nanostructure and thermoelectric properties of hydrothermally synthesized La-containing  $\text{Bi}_2\text{Te}_3$  based alloys. *Mater Chem Phys* 2007;103:484–8.
- [91] Zhao XB, Ji XH, Zhang YH, Lu BH. Effect of solvent on the microstructures of nanostructured  $\text{Bi}_2\text{Te}_3$  prepared by solvothermal synthesis. *J Alloy Compd* 2004;368:349–52.
- [92] Deng Y, Zhou X, Wei G, Liu J, Nan C, Zhao S. Solvothermal preparation and characterization of nanocrystalline  $\text{Bi}_2\text{Te}_3$  powder with different morphology. *J Phys Chem Solids* 2002;63:2119–21.
- [93] Gary Wiederrecht P. *Handbook of Nanoscale Optics and Electronics*. Elsevier; 2010. p. 75–6.
- [94] Mamur H, Ahiska R. A review: thermoelectric generators in renewable energy. *Int J Renew Energy Res (IJRER)* 2014;4:128–36.
- [95] Bhuiyan MRA, Mamur H. Review of the bismuth telluride ( $\text{Bi}_2\text{Te}_3$ ) nanoparticle: growth and characterization. *Int J Energy Appl Technol* 2016;3:74–8.
- [96] El-Sadek S. [M.Sc. Thesis] Faculty of Science, Qena, South Valley University; 2004.
- [97] Lamuta A, Cupolillo A, Politano A, Aliev ZS, Babanly MB, Chulkov EV, Pagnotta L. Indentation fracture toughness of single-crystal  $\text{Bi}_2\text{Te}_3$  topological insulators. *Nano Res* 2016;9:1032–42.
- [98] Park D, Park S, Jeong K, Jeong HS, Song JY, Cho MH. Thermal and electrical conduction of single-crystal  $\text{Bi}_2\text{Te}_3$  nanostructures grown using a one step process. *Nat Sci Rep* 2016;6(19132):1–9.
- [99] Gharsallah M, Serrano-Sánchez F, Bermúdez J, Nemes NM, Martínez JL, Elhalouani F, Alonso J. Nanostructured  $\text{Bi}_2\text{Te}_3$  prepared by a straight forward arc-melting method. *Nanoscale Res Lett* 2016;11:142.
- [100] Elahi SM, Nazari H, Dejam L, Gorji HR. Studying thermoelectric power behaviors of  $\text{Bi}_2\text{Te}_3$  nanoparticles prepared by thermal evaporation. *Open. J Appl Sci* 2016;6:336–42.
- [101] Sie FR, Kuo CH, Hwang CS, Chou YW, Yeh CH, Lin YL, Huang JY. Thermoelectric performance of n-type  $\text{Bi}_2\text{Te}_3/\text{Cu}$  composites fabricated by nanoparticle decoration and spark plasma sintering. *J Electron Mater* 2016;45:1927–34.
- [102] Lin YH, Lin SF, Chi YC, Wu CL, Cheng CH, Tseng WH, He JH, Wu CI, Lee CK, Lin GR. Using n and p type  $\text{Bi}_2\text{Te}_3$  topological insulator nanoparticles to enable controlled femtosecond mode locking of fiber lasers. *ACS Photonics* 2015;2:481–90.
- [103] Chen L, Zhao Q, Ruan X. Facile synthesis of ultra-small  $\text{Bi}_2\text{Te}_3$  nanoparticles, nanorods and nanoplates and their morphology dependent Raman spectroscopy. *Mater Lett* 2012;82:112–5.
- [104] Frantz C, Stein N, Gravier L, Granville S, Boulanger C. Electrodeposition and characterization of bismuth telluride nanowires. *J Electron Mater* 2010;39:2043–8.
- [105] Humphry-Baker Samuel A, Schuh CA. Suppression of grain growth in nanocrystalline  $\text{Bi}_2\text{Te}_3$  through oxide particle dispersions. *J Appl Phys* 2014;116:173505.
- [106] Barman SC, Saha DK, Mamur H, Bhuiyan MRA. Growth and description of Cu nanostructure via a chemical reducing process. *J Nanosci Nano Eng Appl* 2016;6(3):27–31.
- [107] Bhuiyan MRA, Alam MM, Momin MA, Rahman MK, Saha DK. Growth and characterization of  $\text{CuInSe}_2$  nanoparticles for solar cell applications. *J Altern Energy Sources Technol* 2014;5(1):13–7.
- [108] Bhuiyan MRA, Alam MM, Momin MA, Mamur H. Characterization of Al doped ZnO nanostructures via an electrochemical route. *Int J Energy Appl Technol* 2017;4(1):28–33.
- [109] Bhuiyan MRA, Rahman MK. Synthesis and characterization of Ni doped ZnO nanoparticles. *Int J Eng Manuf* 2014;3:67–73.
- [110] Ong CB, Ng LY, Mohammad AW. A review of ZnO nanoparticles as solar photocatalysts: synthesis, mechanisms and applications. *Renew Sustain Energy Rev* 2018;81:536–51.
- [111] Guan H, Hou H, Li M, Cui J. Photocatalytic and thermoelectric properties of  $\text{Cu}_2\text{MnSnS}_4$  nanoparticles synthesized via solvothermal method. *Mater Lett* 2017;188:319–22.
- [112] Gupta B, Melvin AA.  $\text{TiO}_2/\text{RGO}$  composites: its achievement and factors involved in hydrogen production. *Renew Sustain Energy Rev* 2017;76:1384–92.
- [113] Fan Z, Meng F, Zhang M, Wu Z, Sun Z, Li A. Solvothermal synthesis of hierarchical  $\text{TiO}_2$  nanostructures with tunable morphology and enhanced photocatalytic activity. *Appl Surf Sci* 2016;360:298–305.
- [114] Leong KY, Ahmad KK, Ong HC, Ghazali MJ, Baharum A. Synthesis and thermal conductivity characteristic of hybrid nanofluids—a review. *Renew Sustain Energy Rev* 2017;75:868–78.
- [115] Takashiri M, Kai S, Wada K, Takasugi S, Tomita K. Role of stirring assist during solvothermal synthesis for preparing single-crystal bismuth telluride hexagonal nanoplates. *Mater Chem Phys* 2016;173:213–8.
- [116] Ananthakumar S, Ramkumar J, Babu SM. Semiconductor nanoparticles sensitized  $\text{TiO}_2$  nanotubes for high efficiency solar cell devices. *Renew Sustain Energy Rev* 2016;57:1307–21.
- [117] Li Z, Li X, Zong Y, Tan G, Sun Y, Lan Y, He M, Ren Z, Zheng X. Solvothermal synthesis of nitrogen-doped graphene decorated by superparamagnetic  $\text{Fe}_3\text{O}_4$  nanoparticles and their applications as enhanced synergistic microwave absorbers. *Carbon* 2017;115:493–502.
- [118] Yan S, Fu L, Li K, Wang B, Xu X, Xiao L. Solvothermal synthesis of  $\text{SnS}_2/\text{Gold}$  nanoparticle hybrids and their application in non-enzymatic hydrogen peroxide sensing. *Nanosci Nanotechnol-Asia* 2017;7(1):51–7.
- [119] Tzitzios V, Kostoglou N, Giannouri M, Basina G, Tampaxis C, Charalambopoulou G, Steriotis T, Polychronopoulou K, Doumanidis C, Mitterer C, Rebholz C. Solvothermal synthesis, nanostructural characterization and gas cryo-adsorption studies in a metal-organic framework (IRMOF-1) material. *Int J Hydrog Energy* 2017;42(37):23899–907.
- [120] Devendiran DK, Amirtham VA. A review on preparation, characterization, properties and applications of nanofluids. *Renew Sustain Energy Rev* 2016;60:21–40.